IEEE Access
Multidisciplinary | Rapid Review | Open Access Journal

Received September 21, 2019, accepted October 24, 2019, date of publication October 29, 2019,
date of current version November 11, 2019.

Digital Object Identifier 10.1109/ACCESS.2019.2950146

Evaluation of Data Telemetry for Future Leadless Cardiac Pacemaker

PRITAM BOSE[1,2], ALI KHALEGHI[1,3], (Senior Member, IEEE), SALMAN MAHMOOD[2,4], MOHAMMAD ALBATAT[1,2], JACOB BERGSLAND[1,5], AND ILANGKO BALASINGHAM[1,3], (Senior Member, IEEE)

[1]Intervention Center, Oslo University Hospital, 0027 Oslo, Norway
[2]Faculty of Medicine, University of Oslo, 0315 Oslo, Norway
[3]Department of Electronic Systems, Norwegian University of Science and Technology, 7491 Trondheim, Norway
[4]Ovesco Endoscopy AG, 72076 Tübingen, Germany
[5]BH Heart Center, Tuzla 75000, Bosnia and Herzegovina

Corresponding author: Pritam Bose (pritam.bose@studmed.uio.no)

This work was supported by the European Union's H2020: MSCA: ITN Program for the Wireless In-body Environment Communication—WiBEC Project under Grant 675353.

ABSTRACT Multi-node leadless pacemaker system overcomes the main limitations related to lead complications of the conventional cardiac pacemaker and will thus replace them in the near future. The multiple nodes of the technology require the development of low-power, low data-rate and energy-efficient communication framework for device synchronization and bi-directional communication between them. Moreover, the nodes need to communicate with the outer peripheral devices for data telemetry, control and remote monitoring. This paper focuses on evaluation of different energy-efficient modulation schemes at 433 MHz for bi-directional communication between the nodes using homogeneous liquid phantom model of human heart and living animal experiments. In this paper, we have analyzed three simple, low-budget modulation schemes - On Off-Keying (OOK), Frequency Shift-Keying (FSK), and Gaussian Frequency Shift-Keying (GFSK). The analysis is done based on the total transmitter power required to achieve a reliable communication indicated by the minimum threshold values of bit-error rate and packet-error rate. The experiments have been conducted for three common implant communication scenarios - in-body to in-body, in-body to on-body and in-body to off-body links. For conducting the experiments, we have designed the experimental setup with electronic components and fabricated antennas. The results have shown that GFSK has the best performance among the other modulation techniques based on the total transmitter power. We also investigated higher order of the same modulation schemes – 4-FSK and 4-GFSK. The results showed that GFSK performed much better than 4-FSK and 4-GFSK. This research will be carried forward to build the entire radio frequency communication framework for the multi-node pacemaker technology.

INDEX TERMS Implants, pacemakers, wireless communication, radio transceivers, body sensor networks.

I. INTRODUCTION

The multi-node leadless cardiac pacemaker is an innovative technology that can replace the widely used pacemaker technology with leads [1]. They can eliminate the lead-related complications [2]–[5]. There are currently two commercially available leadless pacing systems: the Nanostim leadless cardiac pacemaker (LCP) device (St. Jude Medical, Sylmar, California) [6] and the Micra Transcatheter pacing system (TPS) (Medtronic, Minneapolis, Minnesota) [7]. Both these technologies offer single-chamber stimulation but the technology providing multi-chamber stimulations and cardiac resynchronization will be an optimum solution [8], [9]. Recent research has introduced the multi-nodal leadless pacemaker technology architecture (see Fig. 1) [10]–[13]. The cardiac implants which will hereinafter be called capsules will be equipped with radio frequency (RF) modules to communicate between them (see Fig. 1). RF wireless technology is used for transmission of data packets from transmitter to receiver as it is the most well-researched implant communication technology due to the ease of designing miniaturized and power-efficient systems. The subcutaneous implant S1 can act as a master hub for the capsules C1, C2 and C3 placed inside the heart. The data collected by the sensors present

The associate editor coordinating the review of this manuscript and approving it for publication was Jenny Mahoney.

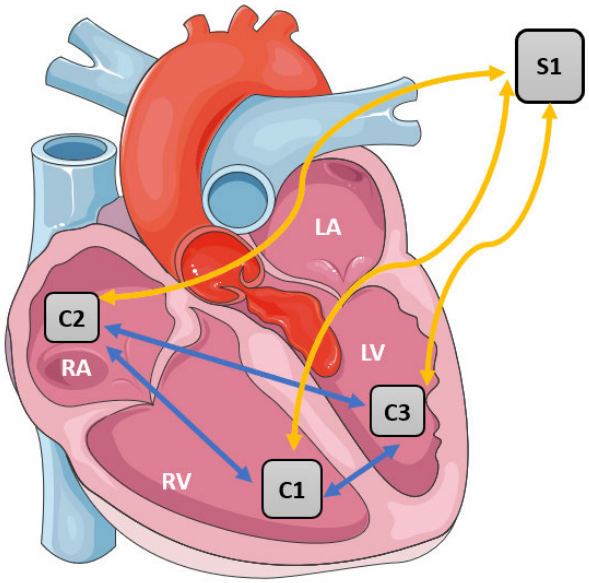

FIGURE 1. Schematic of a three-node leadless capsule pacemaker application for cardiac resynchronization therapy. The capsules C1, C2 and C3 are placed inside the chambers of the heart and they can communicate with the subcutaneous implant S1. RA- right atrium, RV- right ventricle, LA- left atrium, LV- left ventricle, C- capsules and S- subcutaneous implant [10]–[12].

in C1, C2 and C3 can be sent to S1 for decision making. S1 can also act as data storage module and a relay node for communicating with the outside world. The data could be downloaded wirelessly from S1 to outer peripheral devices like phones, computers, etc. for data analysis, device monitoring and configuration changes.

The capsules will have battery to power their electronic circuitries. The two most important requirements for such implant technology are reliable communication and energy efficiency. To have a reliable communication, the bit-error rate (BER) or packet-error rate (PER) should remain below a threshold (BER $< 10^{-4}$). BER is a widely used metric for quality and performance analysis of a communication system which is defined as the ratio of total number of erroneous bits received to the total number of received bits [14]. PER is the ratio of the number of erroneous packets to the total number of received packets. These error rates are functions of several factors, including susceptibility to noise and interference, susceptibility to fading, and non-linearities, which can arise due to dependencies on signal frequency and amplitude.

The receiver capsule should be able to decode all the necessary information from the received bits to make proper decisions. Moreover, the device should be highly energy efficient to prolong the lifetime of the technology. Since, the capsules will be placed inside the heart, it will be difficult to replace them if the battery runs out. The capsule-battery energy consumption is a combination of energy consumed by the electronics and the energy required to transmit data from one capsule to another.

Data rate is not a concern for the capsule pacemaker technology since the sensors (electrogram and accelerometer) in each capsule generates no more than 4.8 Kbits of data per second [15]. This data rate will vary slightly based on the heart rate and the heart movements. Moreover, the transmission distance between the capsules is also quite small (between 5-15 cm) as they are placed inside the body. In traditional communication systems in free space, the transmission energy is dominant compared to the circuit power consumption as the RF signals must travel longer distances. Whereas, for body area networks, the transmission distance is small, so the transmission energy could be comparable to the circuit power consumption. This requires the use of energy-efficient modulation scheme that has also low complexity resulting in simpler electronic design. This would result in less energy consumption which will in turn prolong the battery life of the capsules.

The primary contribution of the paper is the feasibility study of using RF communication inside the heart chambers for the multi-nodal leadless cardiac pacemaker. For the very first time in literature, we determine the optimum RF modulation scheme for bi-directional wireless connectivity between leadless pacemaker devices, based on experiments in liquid phantom and living animal. The RF modulation schemes are elaborated for all three possible implant communication scenarios: in-body to in-body, in-body to on-body and in-body to off-body communication. The secondary contributions of the paper are design, fabrication, and integration of the in-body miniaturized antennas with the electronic systems to explore a realistic pacemaker test scenario in phantom and animal experiments.

In this paper, we analyze three different modulation schemes- On Off-Keying (OOK) [16], Frequency Shift-Keying (FSK) [17] and Gaussian Frequency Shift-Keying (GFSK) [18] at 433 MHz. For the sake of power consumption and circuit complexity, we analyze these three simple modulation schemes. These modulation schemes are not the most spectrally efficient nor do they have the lowest SNR requirements [19]. OOK is the simplest digital modulation that has been used in wireless telemetry bio-devices and biomedical implanted devices [16] as in OOK, binary 0 is represented by no carrier during the transmission which minimizes the power consumption of the modulator. FSK is one of most suitable modulation techniques for low power applications [17]. OOK and FSK are widely used in low-power transceivers since they are phase independent and can be detected by non-coherent architectures which consumes much less power and are less complex compared to coherent-detectors. Implementing a data modulator with low power consumption in wireless transceivers is of interest as the power budget is limited in implantable devices where long battery lives are essential.

The other modulation schemes like PSK, QPSK and DPSK are not chosen because they are phase dependent and require coherent detection which consumes much higher power and the architectures are more complex compared to non-coherent detectors required for OOK, FSK and GFSK.

Quadrature Amplitude Modulation (QAM) is also not chosen because it is used to carry higher data rates compared than ordinary amplitude modulated schemes and phase modulated schemes. This is not required in our case since the multi-node leadless pacemaker is a low data-rate application. Moreover, QAM is more susceptible to noise because the states are closer together resulting in increased required transmitter power to achieve reliable communication.

GFSK modulation utilizes a Gaussian filter to smooth positive/negative frequency deviations and increases the spectral efficiency of a communication system [19]. In principal, the selection of the modulation scheme depends on the system power constraints, accepted complexity in both transmitter and receiver, and the wave propagation channel characteristics [20]. For the leadless pacemaker application, the power efficiency of the system has higher priority compared to other factors like bandwidth efficiency, cost efficiency, etc.

OOK is sensitive to the amplitude fluctuations of the channel, due to the data transmission in the signal amplitude, whereas FSK modulation is more sensitive for the frequency offsets between the transmitter and the receiver [21], [22]. Thus, FSK is commonly used in applications where the frequency accuracy cannot be guaranteed [23]. The heart dynamics with blood perfusion might cause relative movements among the leadless capsules and possible Doppler effects that might shift the frequency and the variable link gain can cause amplitude variations. Therefore, it is important to analyze these simple modulation schemes for the cardiac channel.

FSK modulation creates high level spurious contents as well as relatively high side lobes on the transmitter side, which can cause regulation standard violations. Therefore, GFSK modulation which contains a Gaussian filter can be applied to the symbols before creating the frequency modulated signal to suppress these spurs and side lobes by smoothing the baseband signal [24]. In this paper, we also analyze the performance of higher-order modulation schemes- 4-GFSK and 4-FSK [25], [26]. 2-GFSK modulation is more spectrally efficient than OOK or 2-FSK as the Gaussian filter suppresses the spurious contents and side lobes on the transmitter side significantly while the receiver sensitivity is just slightly worse than 2-FSK and a few dB better than 4-GFSK [27], [28]. Theoretical performance analysis of the modulation schemes is easier in free space whereas extremely challenging for human body environments as human body is a very complex medium consisting of different frequency dependent tissues with varying dielectric properties. Moreover, it will be influenced by body movements and the size of the human body. So, practical in-vivo experiments can only help us to analyze the performance of these modulation schemes in human body environment.

The analysis is done based on the total transmitter power consumption required to achieve a reliable communication at 433 MHz. We have selected 433 MHz for the analysis because it lies in the Industrial, Scientific and Medical (ISM) band [29] which is an unlicensed band and as the name suggests, available for industrial, scientific and medical purposes. Compared to 868 MHz and 2.4 GHz ISM frequency bands, the 433 MHz ISM band has better propagation characteristics because of its lower operating frequency and is currently less affected by external interferences because of the lower number of systems operating in the band [30]. Moreover, the leadless cardiac pacemaker will be short range, low power and low data rate communication systems, so the interference from other communicating systems operating in these bands will be minimum. This will be also helpful in providing physical layer security for the application as it is a highly sensitive device that needs to be completely secured from eavesdropping.

The paper is organized as follows: Section II illustrates the electronic components and antennas fabricated for the study. Phantom and living animal experimental setups are shown in Section III, followed by description of experimental results in Section IV. Finally, concluding remarks and future directions are expressed in Section V.

II. MATERIALS

The hardware setup for conducting the phantom and animal experiments mainly consisted of two categories – the hardware components and the antennas. The hardware components were mostly assembled whereas the antennas were designed and fabricated in our laboratory.

A. HARDWARE COMPONENTS

We use C1200 RF transceiver from Texas Instruments to test the different modulation schemes at 433 MHz [31]. They are integrated single-chip radio transceivers designed for high performance at very low-power and low-voltage operation in cost-effective wireless systems. The C1200 transceivers are mounted on the two SmartRF Transceiver evaluation boards manufactured by Texas Instruments [32]. One is used as transmitter (TxEB) and the other one as receiver (RxEB). They are motherboards that allow the testing of low power RF transceiver devices and the boards can be controlled using SmartRF Studio software [33]. The assembled setup is shown in Fig. 2.

The analysis of total transmitter energy consumption depends on the on-time (Ton) of the transmitter. Ton in turn depends on the data size and the packet size. When the data for each heartbeat is transmitted, the radio goes from sleep mode to active mode. The average wakeup time of the radio is 268μs [34]. This greatly improves the lifetime of the battery as the current consumption during sleep mode (0.12μA) is negligible when compared to that of active mode (46mA at 14dBm) [33]. Though, the radio consumes some additional current to get back to active mode from the sleep mode (1.5mA), the current consumption is very small compared to active mode power consumption and the process is also very fast (133μs). The circuit current consumption increases with the increase in the transmitted signal power (see Fig. 3) [35]. As shown in Fig. 3, the average power consumption is quite high in all the different transmitter power levels because the

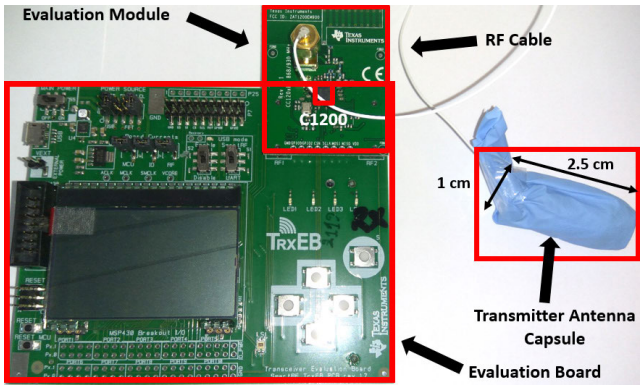

FIGURE 2. The electronic setup of the transmitter. Transmitter Evaluation board (EB) [32] supports the testing of different evaluation modules. The 433 MHz transmitter and receiver evaluation module (EM) supports the testing of different modulation schemes at 433 MHz. The radio chip C1200 in the transmitter capsule setup module is of size 5mm by 5 mm. The 433 MHz evaluation module (EM) is connected to the evaluation board (EB) by placing it appropriately in the grooves. The transmitter antenna is connected to the EM using RF cable.

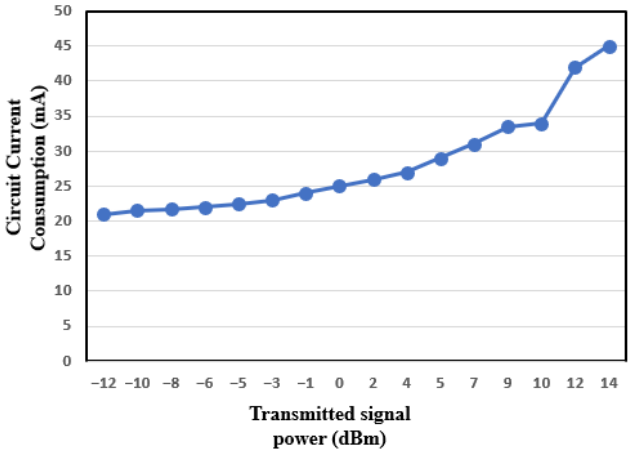

FIGURE 3. The variation of the circuit power consumption (mA) with the transmitted signal power (dBm). It can be seen the circuit power consumption increases with increase in transmitted signal power.

device has too many functionalities that are not applicable for our purpose. It should be mentioned that C1200 transceiver is only used for the evaluation of different modulation schemes and not for the final approval in the leadless pacemaker. Once the optimum parameters have been found, a transceiver IC will be designed that will have much lower power consumption than the current device.

B. ANTENNAS

The implant antenna is a small antenna of size 10 mm × 9 mm designed to be operating at 433 MHz (see Fig. 4a). The wavelength (λ) in free space is 650 mm, therefore the antenna size compared to the wavelength is about $\lambda/65$. The antenna is miniaturized by using the meander line technique in which the antenna electric length is increased, and the antenna matching is conducted by using a capacitive feed mechanism to tune the antenna input resistance to the source 50-ohm impedance. Using the proposed antenna geometry and by tuning the antenna radiation resistance the antenna radiation efficiency inside the biological tissues can be increased [36]. The antenna can be integrated on the surface of a pacemaker metal capsule with little effect from the casing. The antenna holds a superstrate of thickness of 0.7 mm to keep a distance from the surrounded biological tissues. This gap is essential for an efficient antenna operation. The antenna has conformal geometry and is placed on the metal capsule cylinder emulating the pacemaker capsule casing. The antenna is measured in free space and inside the liquid phantom mimicking the material properties of the human body at 433 MHz. Fig. 4b shows the antenna S-parameter in free space and inside the liquid phantom. The S11 is less than −8 dB at 433 MHz.

A pair of the capsule antennas are used in the phantom and animal experiment for evaluating the coupling between the antennas. This test is used to evaluate the capsule to capsule communication quality for synchronous operation of the implants. One of the communication links in the pacemaker technology is to download the capsule's data for diagnostic and programming by a physician. For this purpose, it is required to establish the communication link between the capsule and an the on-body antenna. The on-body antenna can send data signal to place the capsule in the programming mode and download the capsules' memory. A loop type antenna of diameter 50 mm is used in this experiment (see Fig. 5a) [36]. The loop antenna has better EM wave penetration inside biological tissues due to non-magnetic material of the living tissues. The loop antenna impedance is adjusted by using a meander geometry. The antenna is wideband due to the possible mismatching in the application on different human subjects. Fig.5b shows the s-parameters of the on-body antenna measured on the chest of a human subject. The antenna is self-matched thus, it does not need matching circuit for operation. The antenna will be placed directly on the patient's body surface. By using this approach, the near field coupling between the antenna and the implant capsule can be established using smaller transmitter power.

The future pacemakers need to communicate with a remote hub to transmit the capsule data to a patient's network [37]. So, the events can be logged to the network for real time monitoring or supervision of a patent by a physician. This link requires a communication between the capsule and a remote home receiver. An off-body antenna is designed for this purpose. The antenna is wideband and has circular polarized radiation pattern to compensate for the random orientations of the capsule and patient. The antenna operates at 433 MHz with a gain of about 8 dBi. We have studied the performance of such a remote link but at smaller distance. In realistic scenarios, the antenna will be paced more than 2 meters from the patient body to monitor the received signal level.

III. METHODOLOGY

The schematic of the communication system is shown in Fig. 6. The radio in the evaluation board is controlled using the SmartRF Studio software developed by

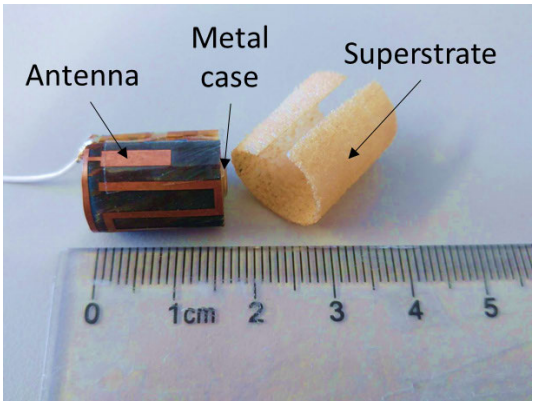

(a)

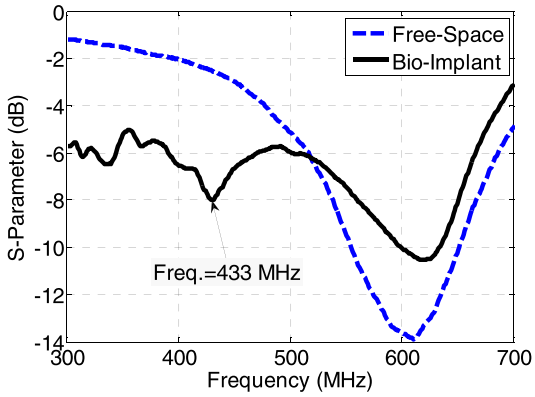

(b)

FIGURE 4. a) Heart implant antenna of size 10 mm by 9 mm b) S11 parameter of the antenna in both free space and biological tissues.

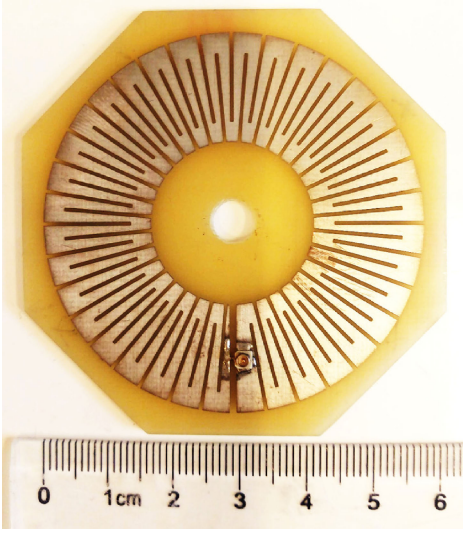

(a)

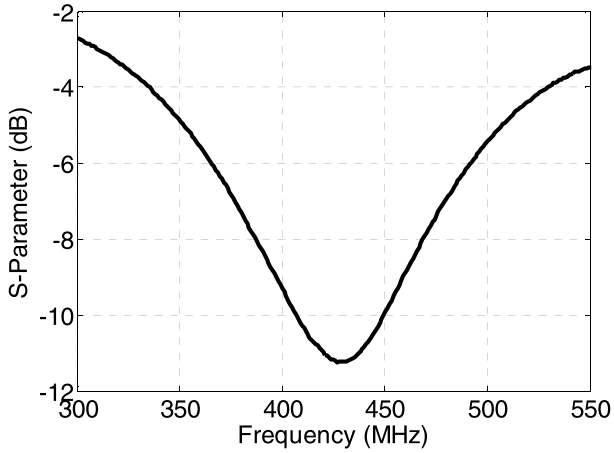

(b)

FIGURE 5. a) On body loop antenna of size 50 mm by 50 mm b) S11 parameter of the antenna.

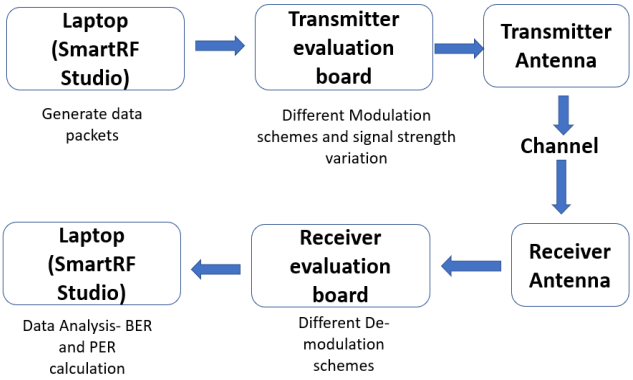

FIGURE 6. Schematic of the communication scheme. The schematic is similar for all the communication scenarios (in-body, on-body and off-body), but the channel will vary depending on the type of scenarios.

Texas Instruments. The board is connected to the PC by a USB cable. We can enter the pilot data to be send in the graphical user interface of the software and select the modulation scheme to be evaluated. We also need to consider the delay requirements as too long data could not be transmitted within the time-window available for data telemetry. The decision making at the subcutaneous hub should be real-time due the critical nature of the medical device.

Bi-directional, half-duplex connection is established between the transmitter (Tx) and the receiver (Rx) antennas. The link power budget [38] can be expressed as:

$$P_{Rx} = P_{Tx} + G_{Tx} + G_{Rx} - L, \quad (1)$$

where P_{Rx} is the power received by Rx antenna in dBm, P_{Tx} is the power transmitted by the Tx antenna in dBm, G_{Tx} and G_{Rx} are the gains of the Tx and Rx antennas in dB respectively and L is the total of all the losses during transmission. The link power budget help us to estimate the amount of loss that a datalink (transmitter to receiver) can tolerate in order to provide a reliable transmission. This is a requirement to set the transmitter with a minimum radiation power for

radiation safety, efficient power consumption and acceptable BER. Moreover, the estimation of the losses will help us better analyze the results, as the changes in channel losses cause changes in BER and PER, resulting in changes in the performance of the system. L can be further expressed as:

$$L = PL + PLF + ML_{Tx} + ML_{Rx}, \quad (2)$$

where PL is the path loss in dB, PLF is the polarization loss factor in dB due to the polarization mismatch between the Tx and Rx antennas, ML_{Tx} and ML_{Rx} are the impedance mismatch losses of the Tx and Rx antennas, respectively.

From our earlier work [11], PL for the in-body communication can be estimated by the linear-distance model as:

$$PL = 10n \times d + PL(d_0) + s, \quad (3)$$

and for the off-body communications as logarithmic model:

$$PL = 10n \log(\frac{d}{d0}) + PL(d_0) + s, \quad (4)$$

where n is the pathloss exponent, d is the distance between the Tx and Rx, $d_0 \leq d$ is the reference distance and s is the random scatter around the mean in dB [39]. The parameters determining the pathloss will vary based on the frequency of operation and position of the implant. From mathematical simulations and experimental validations, it has been seen that n lies within 4 to 5 for the in-body networks [11], [40], [41].

For every experiment, a fixed number of 10^4 data packets is sent from the transmitter to the receiver. The total number of packets lost and error in the received bits helped us to calculate the PER and BER. The transmitted signal power is varied for every modulation scheme to record the least amount of transmitted power required for reliable transmission. The communications channel should not be link limited and losses associated with the channel must not cause the incident power level at the receiver to fall below the receiver sensitivity.

A. LIQUID PHANTOM EXPERIMENTS

Liquid phantom solution is used for the experiments. A saline solution of 0.40% that mimics the dielectric properties of average human heart tissues at 433 MHz [42] is realized. The permittivity and conductivity of heart muscle tissues at 433 MHz are 65.3 and 0.98 S/m respectively [43]. The phantom solution was put into small very thin plastic bags and placed in a plastic container of size $35 \times 35 \times 35$ cm^3. The bags were made as flat as possible and stacked over one another. Special care was taken to get rid of air gaps between the phantom bags by flattening them as much as possible. The entire development kit with the transmitter antenna was placed among the phantom liquid bags at required depths. This special arrangement of putting the liquid phantom in plastic bags was made to minimize the possible signal leakage from the transmitter evaluation board to the receiver evaluation board as we are considering very small sensitivity at the receiver up to −110 dBm. This setup also protected the evaluation board from water contact. In the first experiment for the in-body to in-body channel measurements, the transmitter and receiver consists of the same in-body meander implant antenna. The antennas are placed inside the phantom container at the horizontal distance of 15 cm between them (see Fig. 7, 8a). The selected distance is the maximum normal separation between two capsules inside the heart chambers.

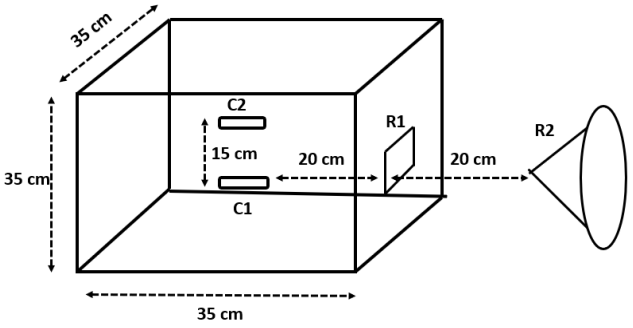

FIGURE 7. Schematic of the phantom experimental setup. The box contains the phantom solution. C1 is implant transmitter capsule, C2 is the implant receiver capsule, R1 is the on-body loop antenna and R2 is the off-body spiral antenna.

The second experiment for the in-body to on-body channel measurements was done between the in-body meander antenna and the on-body loop antenna. The transmitter is connected to the implant and the receiver is the on-body antenna. The distance between Rx and Tx is 20 cm (see fig. 7, 8b). The distance of 20 cm is the logical distance for deep implants from the surface of average human bodies.

The final experiment was done for in-body to off-body channel measurements (see fig. 7, 8c). The in-body meander antenna is the Tx antenna and the off-body antenna is considered as the receiver. The horizontal distance between the antennas is 40 cm with the in-body depth of 20 cm and the off-body distance of additional 20 cm from the body surface.

In all the three experiments, five different modulation schemes: OOK, 2-FSK, 2-GFSK, 4-GFSK and 4-FSK were evaluated based on the average transmitted power. The average received signal strength (Rx power), PER and BER were recorded for each experiment. For each modulation scheme, the transmitted signal power was varied from −16 dBm to 14 dBm and therefore, the communication quality is evaluated. These results helped us to find the optimum modulation scheme for the multi-node pacemaker application based on minimum transmitter power.

B. LIVING ANIMAL EXPERIMENTS

The phantoms experiments are followed by the living animal measurements (see Fig. 9). The experiments were done on a female pig weighing 50.5 kgs. To evaluate and compare the performances of the capsule in an environment like that of the human body, the pig used in this experiment was prepared under a general anesthesia. All studies were performed at the hybrid operating room of the Intervention Centre, Rikshospitalet, Oslo University Hospital, Norway that has accreditation

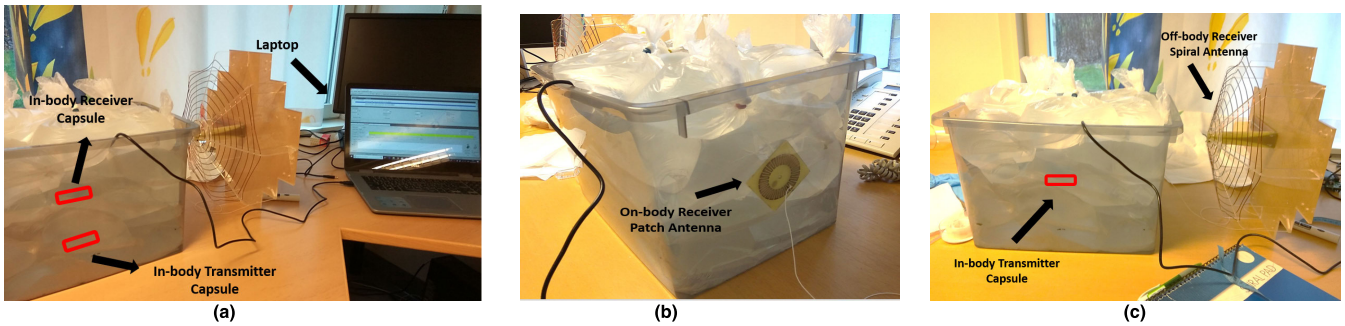

FIGURE 8. a) Phantom experimental setup for in-body to in-body communication. The evaluation boards with the transmitter capsule and receiver capsule have been placed inside the phantom solution and cannot be viewed clearly in the figure but the positions have been marked with red boxes for better visual representation. b) Phantom experimental setup for in-body to on-body communication. The evaluation board with the transmitter capsule has been placed inside the phantom solution whereas the on-body patch antenna is attached to the side of the container c) Phantom experimental setup for in-body to off-body communication. The off-body antenna is aligned in the same horizontal plane of the transmitter capsule.

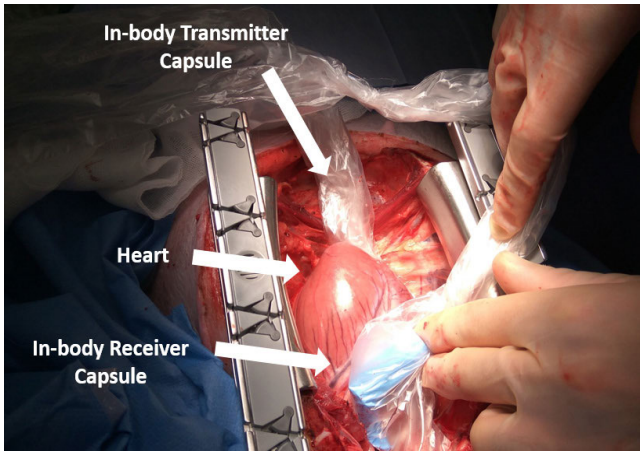

FIGURE 9. Animal experimental setup for in-body to in-body communication. The chest of the pig is cut open to place the capsules. The transmitter capsule is placed beneath the right ventricle (under the heart) and the receiver capsule on the left atrium (over the heart). The chest is then firmly closed with stitches so that there is no leakage of RF signal through the cuts.

for conducting animal experiments. All the experiments were performed in strict compliance with the Norwegian and European Union laws on Ethical standards and humane treatment of animals. Because this animal was alive, and all its organs were operating normally, the experimental conditions were virtually identical to conditions expected in a human body.

The first experiment was done for the in-body to in-body measurements. The implant Tx and Rx antennas were placed on the either side of the heart – Tx outside the right ventricle and the Rx outside the left atrium. The optimal placement would have been inside the heart chambers, but the heart is not punctured to place the implants inside the heart. This is because the current capsule size is slightly bigger compared to our estimated final prototype dimensions and thus to prevent the early death of the animal as it is used for multiple other experiments. The distance between the implants are measured with the help of a magnetic distance measurement system called Medical Aurora manufactured by the company northern Digital Inc. that gives accurate distance measurements. The distance between the implants were found to 5 cm which is smaller than the average pig heart as the pig was few months old.

The second experiment was done for the in-body to on-body measurements. The implant antenna was placed under the right ventricle and the on-body Rx loop antenna on the chest surface. The distance between them was measured to be 8 cm. The final experiment was done for the in-body to off-body measurements. The implant Tx antenna was kept at the same position whereas the off-body spiral antenna was placed at a vertical distance of 40 cm from the surface of the body. The total distance between the Tx and Rx antennas was 48 cm (8 cm inside the body and 40 cm outside the body).

All the experiments were very similar to the phantom experiments. The different modulation schemes were evaluated by varying the transmitted power. The optimum modulation scheme was obtained by analyzing the corresponding Tx power, BER and PER.

IV. RESULTS AND DISCUSSIONS

The data rate has been fixed at 4.8 kbps for all the modulation schemes for all the communication scenarios. The phantom results are plotted in graphs for better visual representation. The animal experiment results are represented in tables due to lower number of available data points.

A. PHANTOM EXPERIMENT RESULTS

The phantom results for the in-body to in-body communication at the distance of 15 cm are shown in Fig. 10. To achieve a reliable communication (PER and BER $< 10^{-4}$), the required Tx power for OOK is very high and beyond the maximum Tx power that can be provided by the evaluation board. At 14dBm, the PER and BER for OOK are -49.1% and 0.93% respectively, which is far away from the PER and BER required for reliable communication. To achieve reliable communication, the Tx power for 2-FSK and 2-GFSK are 13 dBm and 6 dBm respectively. The required power for higher order modulation schemes like 4-FSK and 4-GFSK

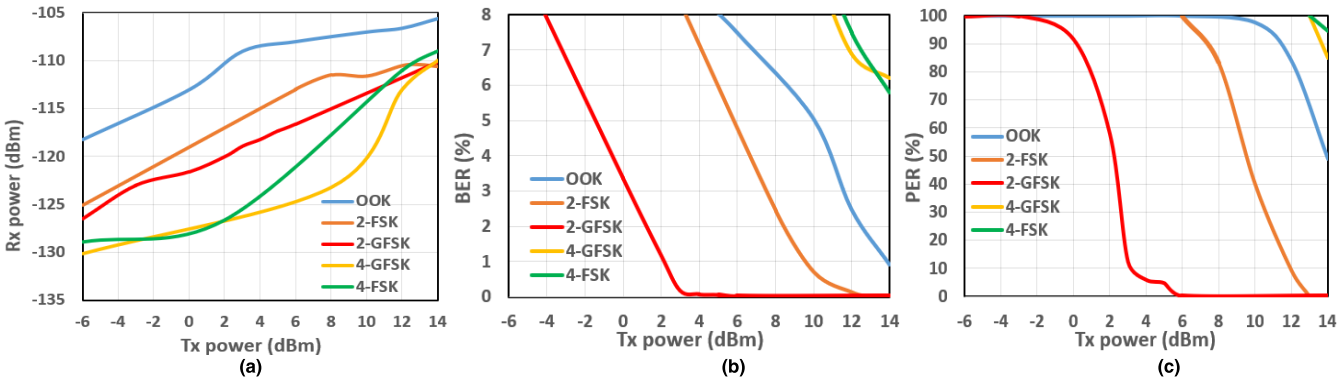

FIGURE 10. Phantom experimental results for in-body to in-body communication. Variations of the a) Rx power with the Tx power b) BER and c) PER for different modulation schemes.

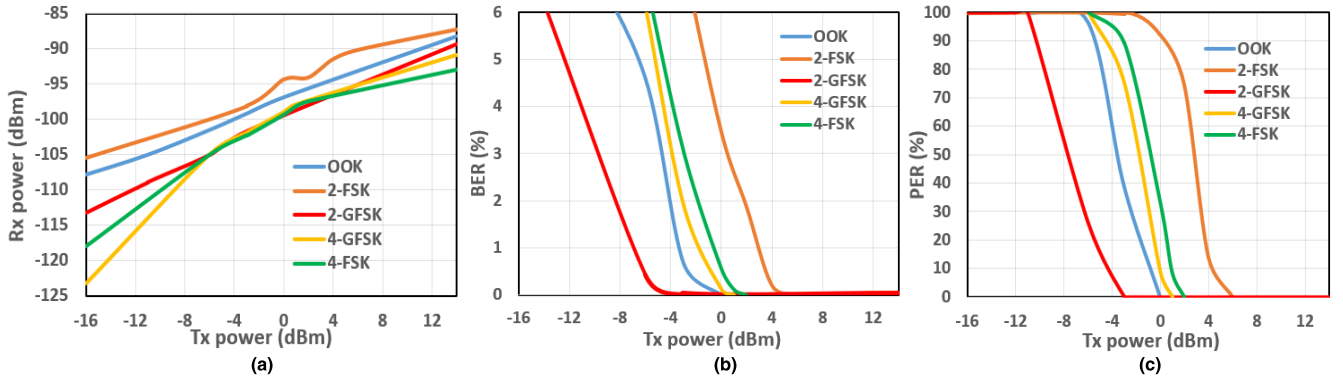

FIGURE 11. Phantom experimental results for in-body to on-body communication. Variations of a) Rx power with the Tx power b) BER and c) PER for different modulation schemes.

to achieve reliable communication are beyond 14 dBm and cannot be exactly computed due to the Tx power constraint of the evaluation board. This shows that the 2-GFSK is the optimum modulation scheme as it requires the least amount of Tx power to achieve reliable communication compared to all other modulation schemes.

All the packets are lost when the Tx power for 2-GFSK is below −3dBm. Whereas for OOK, 2-FSK, 4-FSK and 4-GFSK, PER is 100% when Tx power is 8 dBm, 6 dBm, 13dBm and 13dBm respectively. This shows that the performance of 2-GFSK is better than all the other modulation schemes. It can be seen (see Figs. 10b and 10c) that the PER increases significantly with BER which shows the errors in bits is distributed over the entire data or in other terms, over all the packets. This shows the channel is slow fading and is constant over each time-window of data-transmission. The Rx power not only varies with the Tx power but also with the modulation schemes (see Fig. 10a). OOK has the best Rx power in average followed by 2-FSK, 2-GFSK, 4-FSK and 4-GFSK respectively. We believe this variation mainly occurs from the post-processing done by the evaluation board.

The phantom results for the in-body to on-body communication at 20 cm are shown in Fig. 11. To achieve a reliable communication, the required Tx power for OOK, 2- FSK, 2-GFSK, 4-FSK and 4-GFSK are 0 dBm, 6 dBm, −3 dBm, 2 dBm and 1 dBm respectively. The PER is 100% when the Tx power is less than −6 dBm, −3 dBm, −11 dBm, −6dBm and −6dBm for OOK, 2-FSK, 2-GFSK, 4-FSK and 4-GFSK respectively. Both these results show that 2-GFSK has the best performance just like the previous communication scenario. The phantom results for the in-body to off-body communication at the total distance of 40 cm (in-body distance = 20 cm and off-body distance = 20 cm) are shown in Fig. 12. To achieve a reliable communication, the required Tx power for OOK, 2- FSK and 2-GFSK are 8 dBm, 14 dBm and 7 dBm respectively. The required power for higher order modulation schemes 4-FSK and 4-GFSK to achieve reliable communication are beyond 14 dBm and cannot be exactly computed as the due to the Tx power constraint of the evaluation board. This shows that 2-GFSK is the optimum modulation scheme. The introduction of manual movements on the phantom to simulate the heart movements resulted in decrease of Tx power by 1.5 dB in average and increase in PER and BER for all the modulation schemes. In case of 2-GFSK, this change was the least and it provided the best results among all the modulation schemes. It can be observed that the Rx power is better for in-body to on-body communication (see Fig. 11a) compared to in-body to in-body communication

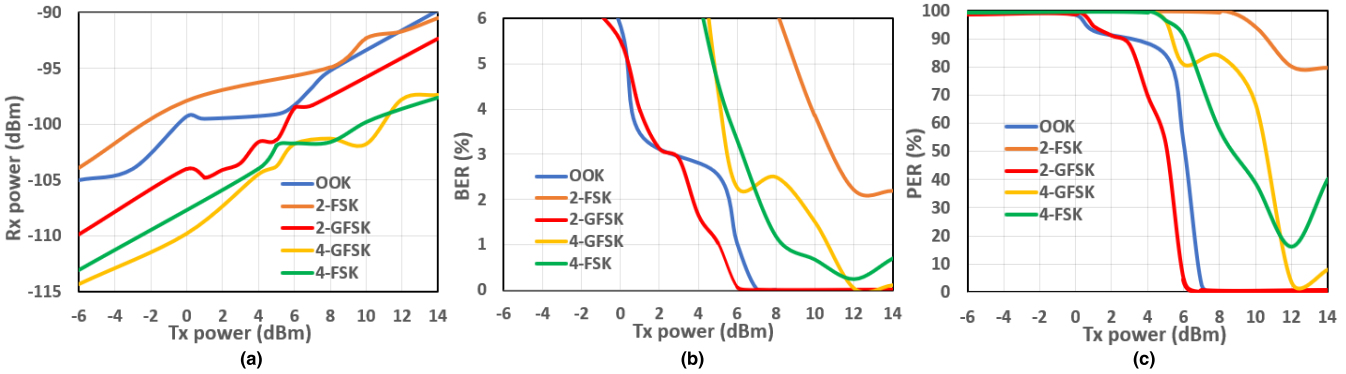

FIGURE 12. Phantom experimental results for in-body to off-body communication. Variations of the a) Rx power with the Tx power b) BER and c) PER for different modulation schemes.

(see Fig. 10a) although the distance between the antennas in the former case is 3 cm more than latter one. This is mainly due to the antenna gain and polarization. The receiver loop antenna for on-body communication has higher gain compared to the receiver meander antenna for in-body communication. Thus, both antenna gains and orientations play a major role in the latter case and any mismatch could cause significant reduction in the Rx power. The in-body to in-body communication link could be improved by designing high-efficiency dual-polarized antenna but it is a challenging task given the size constraints. Thus, designing highly efficient mm-sized implant antennas could be a significant research direction.

B. ANIMAL EXPERIMENT RESULTS

The living animal experiments are conducted to validate the phantom experiments, but the degrees of freedom are limited in the animal experiment. The results for the in-body to in-body communication at 5 cm are shown in Table 1. We notice that for all the modulation schemes, the reliable communication can be performed at Tx power of −24 dBm. At Tx power of −40dBm, the 2-FSK shows no communication and OOK shows communication with very high PER and BER, whereas 2-GFSK shows better communication with lower PER and BER. From the observations, it can be concluded that 2-GFSK performs better than OOK and 2-FSK. The selection of Tx powers between −40 dBm and −24 dBm could provide more concrete results but this cannot be evaluated as the evaluation board only allows to select −40 dBm and −24 dBm of Tx powers at such low Tx powers. This is one of the limitations of this evaluation board. Thus, the required Tx power for 4-GFSK is similar to 2-GFSK and their differences cannot be differentiated. Due to the small size of the heart of the pig, the distance between the in-body antennas cannot also be increased, otherwise more discrete values at higher Tx powers could have been used to have a better evaluation of the modulation schemes. 4-FSK showed the worst results as it required 0 dBm of Tx power to achieve reliable communication.

TABLE 1. Living animal experiment results for in-body to in-body communication.

Modulation Scheme	Tx power (dBm)	Rx power (dBm)	PER (%)	BER (%)
OOK	-40	-106	93.9	3.81
	-24	**-90.7**	**0**	**0**
2-FSK	-40	-104.2	100	-
	-24	**-88.5**	**0**	**0**
2-GFSK	-40	-110.1	32.8	0.55
	-24	**-91.3**	**0**	**0**
4-GFSK	-40	-103.9	100	-
	-24	**-88.6**	**0**	**0**
4-FSK	-40	-104.6	100	-
	-24	-88.4	14.6	0.22
	-12	-75.9	6.9	0.1
	-6	-69.8	5.1	0.09
	-3	-67.1	5.7	0.08
	0	**-64.6**	**0**	**0**

The results for the in-body to on-body communication at a distance of 8 cm are shown in Table 2. To achieve a reliable communication, the required Tx power for OOK, 2- FSK and 2-GFSK are 6 dBm, 14 dBm and 3 dBm respectively. The required power for higher order modulation schemes 4-FSK and 4-GFSK to achieve reliable communication are beyond 14 dBm. This shows that 2-GFSK is the optimum modulation scheme based on Tx power requirement. The results for the in-body to off-body communication at a total distance of 48 cm (inbody = 8 cm and off-body = 40 cm) are shown in Table 3. To achieve a reliable communication, the required Tx power for OOK, 2- FSK and 2-GFSK are 0 dBm, 6 dBm and −6 dBm respectively. The required power for higher order modulation schemes 4-FSK and 4-GFSK to achieve reliable communication are 0 dBm for both. This shows that

TABLE 2. Living animal experiment results for in-body to on-body communication.

Modulation Scheme	Tx power (dBm)	Rx power (dBm)	PER (%)	BER (%)
OOK	0	-105.3	95.5	4.28
	3	-104.8	66.3	1.5
	6	**-103.4**	**0**	**0**
2-FSK	0	-106.1	100	-
	6	-101.9	100	-
	10	-96.6	42.3	0.77
	14	**-95.1**	**0**	**0**
2-GFSK	-6	-114	100	-
	-3	-111	89.7	3.17
	0	-109.7	61.7	1.33
	3	**-107.7**	**0**	**0**
4-GFSK	0	-105.2	100	-
	6	-99	100	-
	10	-99	96.3	4.47
	14	**-94.3**	**81**	**2.28**
4-FSK	6	-101	100	-
	10	-97	96.6	4.57
	14	**-94.3**	**87.4**	**2.84**

TABLE 3. Living animal experiment results for in-body to off-body communication.

Modulation Scheme	Tx power (dBm)	Rx power (dBm)	PER (%)	BER (%)
OOK	-12	-111	100	-
	-6	-102	7.1	0.1
	0	**-96.4**	**0**	**0**
2-FSK	-6	-101.7	100	-
	0	-95	38.6	0.67
	6	**-89**	**0**	**0**
2-GFSK	-12	-109	100	-
	-6	**-104.1**	**0**	**0**
4-GFSK	-12	-109	100	-
	-6	-104.4	17.3	0.26
	-3	-101.7	2.8	0.04
	0	**-98.3**	**0**	**0**
4-FSK	-12	-110	100	-
	-6	-104	29.5	0.48
	0	**-98.4**	**0**	**0**

2-GFSK has the best performance like the previous communication scenarios.

Both the phantom and the living animal experiments concluded GFSK as the optimum modulation scheme among the evaluated ones based on the least Tx power required. This is also true for all the possible communication scenarios. One of the primary reasons for the better performance of GFSK compared to the other modulation techniques is that it has very good tolerance to the inter-symbol interference when the system is operating at relatively low-data rate. GFSK uses a smaller part of the spectrum and therefore waste less power. It also makes the signal less susceptible to amplitude nonlinearities introduced by the channel and/or receiver hardware.

Moreover, Gaussian filters in GFSK have advantages in terms of carrier power, occupied bandwidth and symbol clock recovery. It is Gaussian in shape in both the time and frequency domain. Its effects in the time domain are relatively short and each symbol interacts with only the preceding and succeeding symbols. This reduces the tendency for sequences of symbols to interact which makes amplifiers easier to build and more efficient resulting in simpler and power efficient communication system design. Increase in transmitted signal power level not only increases the power output of the circuit but also causes increase in the circuit current consumption (see Fig. 3). So, more battery will be drained out in case of higher transmitted power to achieve reliable communication.

Both the phantom and the living animal experiments also confirmed that lower order modulation schemes perform much better than higher order modulation schemes in terms of the transmitted power requirement. Higher order modulation schemes increase the spectral efficiency, but unfortunately as spectral efficiency increases, so does the error rates, which means a higher SNR might be needed to achieve acceptable error rates for reliable communication. Moreover, higher order modulation and demodulation schemes requires more complex hardware, which is difficult to implement, and the circuit power consumption also increases.

It can be observed from the results that though all the experiments confirmed GFSK as the optimum modulation scheme, but the Rx power varied significantly not only between the phantom and animal experiments but also between the different communication scenarios. This is mainly due to the post-processing done by the evaluation board and antenna effects like impedance mismatch of the antennas, antenna rotation, polarization mismatch and misalignment of the antenna. Moreover, the receiver antennas used for the three different communication scenarios were different due to the size constraints. The size of the implant antenna had to be significantly smaller as compared to the on-body and off-body antennas due to the limited size of the capsule pacemaker can.

It can be seen from both the phantom and the animal experiments that the Tx power requirement is quite high for an in-body implant scenario which will deplete the battery in short time duration. This is due to the multi-functionalities of the C1200 transceiver IC which are not applicable for our purpose and won't be included in the final prototype.

The experiments have provided us with some of the optimum parameters required for developing the final prototype. Once most of the optimum parameters for the prototype has been found, a transceiver IC will be designed that will have much lower power consumption than this current IC.

V. CONCLUSION AND FUTURE WORK

In this paper, the modulation schemes for the communication system design at 433 MHz for the multi-node leadless pacemaker have been analyzed. We have used the evaluation boards combined with fabricated antennas for the experiments. The analysis is done based on liquid phantom solutions that mimics the dielectric properties of human heart tissues at 433 MHz and living animal experiments. This gives us more realistic results compared to theoretical simulations.

We have found out that GFSK is the optimum modulation scheme due to its high tolerance to interference at low data rates. We also found out 2-GFSK performs better than 4-GFSK and 4-FSK which shows that lower order modulation schemes offer better results compared to higher order modulation schemes.

The next goal is to fabricate the evaluation module on a very small printed circuit board (PCB). This will help us to assemble the entire pacemaker setup in a small capsule. This capsule can then be placed inside the chambers of the heart to have more realistic results. This could not be done in the beginning as multiple scenarios cannot be tested using a single PCB. Since we have a fair idea about the optimum settings for the pacemaker module now, we can fabricate the PCB with these optimum settings. The other goal is to perform similar experiments at other ISM frequencies – 868 MHz and 2.4 GHz, to have a comparison of the results with 433 MHz. This work has provided us a strong foundation towards the design of the complete prototype of the multi-node pacemaker system.

REFERENCES

[1] M. O. Sweeney, A. Hellkamp, and K. Ellenbogen, "Adverse effect of ventricular pacing on heart failure and atrial fibrillation among patients with normal baseline QRS duration in a clinical trial of pacemaker therapy for sinus node dysfunction," *Circulation*, vol. 107, no. 23, pp. 2932–2937, Jun. 2003.

[2] M. S. Kiviniemi, M. A. Pirnes, H. J. K. Eränen, R. V. J. Kettunen, and J. E. K. Hartikainen, "Complications related to permanent pacemaker therapy," *Pacing Clin. Electrophysiol.*, vol. 22, no. 5, pp. 711–720, May 1999.

[3] A. A. Harcombe, S. A. Newell, P. F. Ludman, T. E. Wistow, L. D. Sharples, P. M. Schofield, D. L. Stone, L. M. Shapiro, T. Cole, and M. C. Petch, "Late complications following permanent pacemaker implantation or elective unit replacement," *Heart*, vol. 80, no. 3, pp. 240–244, Jan. 1998.

[4] K. G. Tarakji, O. M. Wazni, S. Harb, A. Hsu, W. Saliba, and B. L. Wilkoff, "Risk factors for 1-year mortality among patients with cardiac implantable electronic device infection undergoing transvenous lead extraction: The impact of the infection type and the presence of vegetation on survival," *Europace*, vol. 16, no. 10, pp. 1490–1495, Feb. 2014.

[5] E. O. Udo, N. P. A. Zuithoff, N. M. van Hemel, C. C. de Cock, T. Hendriks, P. A. Doevendans, and K. G. M. Moons, "Incidence and predictors of short- and long-term complications in pacemaker therapy: The FOLLOWPACE study," *Heart Rhythm*, vol. 9, no. 5, pp. 728–735, May 2012.

[6] C.-P. Lau, K. Chen, K.-F. Lee, Y. Dai, and S. Zhang, "Implantation and clinical performance of an entirely leadless cardiac pacemaker," *Int. J. Heart Rhythm*, vol. 1, no. 1, pp. 50–54, Sep. 2016.

[7] E. H. Nichols and P. Ritter, "Micra transcatheter pacing system safe, effective," *MD Conf. Exp.*, vol. 15, no. 22, pp. 8–9, Jan. 2015.

[8] K. Takizawa, T. Aoyagi, J.-I. Takada, N. Katayama, K. Yekeh, Y. Takehiko, and K. R. Kohno, "Channel models for wireless body area networks," in *Proc. 30th Annu. Int. Conf. IEEE Eng. Med. Biol. Soc.*, Aug. 2008, pp. 1549–1552.

[9] L. Bereuter, T. Kuenzle, T. Niederhauser, M. Kucera, D. Obrist, T. Reichlin, H. Tanner, and A. Haeberlin, "Fundamental characterization of conductive intracardiac communication for leadless multisite pacemaker systems," *IEEE Trans. Biomed. Circuits Syst.*, vol. 13, no. 1, pp. 237–247, Feb. 2019.

[10] P. Bose, A. Khaleghi, M. Albatat, J. Bergsland, and I. Balasingham, "RF channel modeling for implant-to-implant communication and implant to subcutaneous implant communication for future leadless cardiac pacemakers," *IEEE Trans. Biomed. Eng.*, vol. 65, no. 12, pp. 2798–2807, Dec. 2018, doi: 10.1109/tbme.2018.2817690.

[11] P. Bose, A. Khaleghi, and I. Balasingham, "In-body and off-body channel modeling for future leadless cardiac pacemakers based on phantom and animal experiments," *IEEE Antennas Wireless Propag. Lett.*, vol. 17, no. 12, pp. 2484–2488, Dec. 2018, doi: 10.1109/lawp.2018.2878950.

[12] P. Bose, A. Khaleghi, and I. Balasingham, "Wireless channel modeling for leadless cardiac pacemaker: Effects ofventricular blood volume," in *Proc. 40th Annu. Int. Conf. IEEE Eng. Med. Biol. Soc. (EMBC)*, Jul. 2018, pp. 3746–3749, doi: 10.1109/embc.2018.8513099.

[13] M. F. Awan, S. Perez-Simbor, C. Garcia-Pardo, K. Kansanen, P. Bose, S. Castelló-Palacios, and N. Cardona, "Experimental phantom-based evaluation of physical layer security for future leadless cardiac pacemaker," in *Proc. IEEE 29th Annu. Int. Symp. Pers., Indoor Mobile Radio Commun. (PIMRC)*, Sep. 2018, pp. 333–339, doi: 10.1109/pimrc.2018.8580808.

[14] J. Dong, "Estimation of bit error rate of any digital communication system," Ph.D. dissertation, Télécom Bretagne, Univ. Western Brittany, Brest, France, 2013.

[15] G. G. Messier and I. G. Finvers, "Traffic models for medical wireless sensor networks," *IEEE Commun. Lett.*, vol. 11, no. 1, pp. 13–15, Jan. 2007.

[16] M. A. Hannan, S. M. Abbas, S. A. Samad, and A. Hussain, "Modulation techniques for biomedical implanted devices and their challenges," *Sensors*, vol. 12, no. 1, pp. 297–319, Jan. 2012.

[17] M. Seyedi, B. Kibret, D. T. H. Lai, and M. Faulkner, "A survey on intrabody communications for body area network applications," *IEEE Trans. Biomed. Eng.*, vol. 60, no. 8, pp. 2067–2079, Aug. 2013.

[18] S. H. Gerez, "Implementation of digital signal processing: Some background on GFSK modulation," Dept. Elect. Eng., Univ. Twente, Enschede, The Netherlands, Tech. Rep., 2013.

[19] J. G. Proakis and M. Salehi, *Digital Communications*, vol. 4. New York, NY, USA: McGraw-Hill, 2001, pp. 593–620.

[20] J. Luo, A. A. Zaidi, J. Vihriälä, D. Giustiniano, Y. Qi, H. Halbauer, D. Ktnas, R. Weiler, H. Miao, and J. Lorca, "Millimetre-wave air-interface for 5G: Challenges and design principles," in *Proc. ETSI Workshop Future Radio Technol.-Air Inter.*, 2016, pp. 1–6.

[21] C. Li, D. A. Hutchins, and R. J. Green, "Short-range ultrasonic digital communications in air," *IEEE Trans. Ultrason., Ferroelectr., Freq. Control*, vol. 55, no. 4, pp. 908–918, Apr. 2008, doi: 10.1109/tuffc.2008.726.

[22] D. Mulally and D. Lefevre, "A comparison of digital modulation methods for small satellite data links," Cynetics Corp., Rapid City, SD, USA, Tech. Rep., 1991.

[23] D. L. Ash, "A comparison between OOK/ASK and FSK modulation techniques for radio links," RF Monothilics Inc, Dallas, TX, USA, Tech. Rep., 1992.

[24] H. J. Bergveld, K. M. M. V. Kaam, D. M. W. Leenaerts, K. J. P. Philips, A. W. P. Vaassen, and G. Wetkzer, "A low-power highly digitized receiver for 2.4-GHz-band GFSK applications," *IEEE Trans. Microw. Theory Techn.*, vol. 53, no. 2, pp. 453–461, Feb. 2005.

[25] S. Georgi, "Wireless transmission system and method of wirelessly transmitting digital information," U.S. Patent 13 221 411, Feb. 28, 2013.

[26] R. I. Seshadri and C. V. Matthew, "A capacity-based search for energy and bandwidth efficient bit-interleaved coded noncoherent GFSK," in *Proc. Virginia Tech Symp. Wireless Pers. Commun.*, 2006, pp. 1–10.

[27] V. Mohan, "An introduction to wireless M-Bus," Silicon Labs, Austin, TX, USA, Tech. Rep., 2015.

[28] R. E. Rouquette, "GFSK receiver architecture and methodology," U.S. Patent 8 625 722, Jan. 7, 2014.

[29] R. Alrawashdeh, Y. Huang, and P. Cao, "Flexible meandered loop antenna for implants in MedRadio and ISM bands," *Electron. Lett.*, vol. 49, no. 24, pp. 1515–1517, Nov. 2013, doi: 10.1049/el.2013.3035.
[30] P. Tuset-Peiró, A. Anglès-Vazquez, J. López-Vicario, and X. Vilajosana-Guillén, "On the suitability of the 433 MHz band for M2M low-power wireless communications: Propagation aspects," *Trans. Emerg. Telecommun. Technol.*, vol. 25, no. 12, pp. 1154–1168, Dec. 2014, doi: 10.1002/ett.2672.
[31] *CC1200 Low-Power, High-Performance RF Transceiver Datasheet*, Texas Instruments, Dallas, TX, USA, 2014.
[32] *TrxEb Development Tool User's Guide*, Texas Instruments, Dallas, TX, USA, 2012.
[33] *SmartRF Studio 7 Tutorial Product (Rev. B)*, Texas Instruments, Dallas, TX, USA, 2011.
[34] G. Daneels, E. Municio, B. Van de Velde, G. Ergeerts, M. Weyn, S. Latré, and J. Famaey, "Accurate energy consumption modeling of IEEE 802.15.4e TSCH using dual-band OpenMote hardware," *Sensors*, vol. 18, no. 2, p. 437, Feb. 2018, doi: 10.3390/s18020437.
[35] S. Barrachina-Muñoz, B. Bellalta, T. Adame, and A. Bel, "Multi-hop communication in the uplink for LPWANs," *Comput. Netw.*, vol. 123, pp. 153–168, Aug. 2017, doi: 10.1016/j.comnet.2017.05.020.
[36] A. Khaleghi, A. Hasanvand, and I. Balasingham, "Radio frequency backscatter communication for high data rate deep implants," *IEEE Trans. Microw. Theory Techn.*, vol. 67, no. 3, pp. 1093–1106, Mar. 2019.
[37] A. K. Teshome, B. Kibret, and D. T. H. Lai, "A review of implant communication technology in WBAN: Progress and challenges," *IEEE Rev. Biomed. Eng.*, vol. 12, pp. 88–99, 2019.
[38] A. Kiourti and K. S. Nikita, "Miniature scalp-implantable antennas for telemetry in the MICS and ism bands: Design, safety considerations and link budget analysis," *IEEE Trans. Antennas Propag.*, vol. 60, no. 8, pp. 3568–3575, Aug. 2012, doi: 10.1109/tap.2012.2201078.
[39] A. Alomainy and Y. Hao, "Modeling and characterization of biotelemetric radio channel from ingested implants considering organ contents," *IEEE Trans. Antennas Propag.*, vol. 57, no. 4, pp. 999–1005, Apr. 2009, doi: 10.1109/tap.2009.2014531.
[40] K. Sayrafian-Pour, "A statistical path loss model for medical implant communication channels," in *Proc. IEEE 20th Int. Symp. Pers., Indoor Mobile Radio Commun.*, Sep. 2009, pp. 2995–2999, doi: 10.1109/pimrc.2009.5449869.
[41] I. Dove, "Analysis of radio propagation inside the human body for in-body localization purposes," M.S. thesis, Dept. Elect. Eng., Univ. Twente, Enschede, The Netherlands, 2014.
[42] D. H. Gadani, V. A. Rana, S. P. Bhatnagar, A. N. Prajapati, and A. D. Vyas, "Effect of salinity on the dielectric properties of water," *Indian J. Pure Appl. Phys.*, vol. 50, pp. 405–410, Jun. 2012.
[43] ITIS Foundation. (2010). *Tissue Properties*. Accessed: Feb. 24, 2019. [Online]. Available: https://itis.swiss/virtual-population/tissue-properties/database/tissue-frequency-chart/

PRITAM BOSE received the B.Tech. degree in electronics and communications engineering from the West Bengal University of Technology, Kolkata, India, in 2013, and the M.Sc. degree in telecommunications engineering from the University of Trento, Trento, Italy, in 2016. He carried out his master thesis with the Knowledge Engineering and Discovery Research Institute (KEDRI), Auckland University of Technology, Auckland, New Zealand. He is currently pursuing the Ph.D. degree with the Department of Clinical Medicine, Faculty of Medicine, University of Oslo. He is also doing his Ph.D. degree research work with the Intervention Centre, Oslo University Hospital, Norway. His research interests include signal processing, channel modeling for body sensor networks, and communication system design for wireless medical technologies.

ALI KHALEGHI (M'02–SM'14) received the Ph.D. degree in physics from the University of Paris XI, Paris, France, in 2006. From 2006 to 2007, he was a Postdoctoral Researcher with the Institute d' Electronique et de Telecommunications de Rennes (IETR), Rennes, France. From 2008 to 2009, he was a Postdoctoral Researcher with the Intervention Center (IVS), Oslo University Hospital, Oslo, Norway. From 2010 to 2015, he was an Assistant Professor with the Electrical and Computer Engineering Department, K. N. Toosi University of Technology (KNTU), Tehran, Iran. He has authored more than 90 journals and full conference papers. He holds six international patents. His current research interests include antenna and wave propagation, wireless communications, electromagnetic compatibility, measurement techniques, and bioelectromagnetics. He was a recipient of several research and industrial grants during his career at KNTU, where he established the Wireless Terminal Test Lab. He was distinguished as the Best Researcher of KNTU, in 2013. Since 2015, he has been an Adjunct Professor with KNTU and a Scientist with the Norwegian University of Science and Technology (NTNU), Trondheim, Norway, and with Oslo University Hospital.

SALMAN MAHMOOD received the bachelor's degree in electrical engineering from the National University of Sciences and Technology, Pakistan, in 2012, and the joint M.Sc. degree in smart system integration from a Tri-University Consortium consisting of Heriot-Watt University, U.K., the University of Southeast Norway, and the Budapest University of Technology and Economics, Hungary, on an Erasmus Mundus Scholarship, in 2015. He is currently pursuing the Ph.D. degree with the Department of Clinical Medicine, Faculty of Medicine, University of Oslo. He is also doing the Ph.D. research work with Ovesco Endoscopy AG, Tuebingen, Germany. He has eight years of industrial experience in electronics design and system automation. His research interests include implantable electronics, ingestible sensors, magnetic actuation, robotics, machine learning, and system integration.

MOHAMMAD ALBATAT received the bachelor's degree in biomedical engineering from the City University London, U.K., in 2014, and the M.Sc. degree in physics and engineering in medicine from the University College London, U.K., in 2015. He is currently pursuing the Ph.D. degree with the Department of Clinical Medicine, Faculty of Medicine, University of Oslo. He is also doing the Ph.D. degree research work with the Intervention Centre, Oslo University Hospital, Norway. He was a Clinical Engineer with NHS, U.K., for a year assuring optimum medical device support throughout Lister hospital.

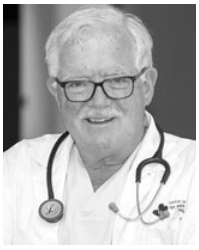

JACOB BERGSLAND received the degree in medical and the Ph.D. degree from Oslo University, in 1973 and 2011, respectively, and the M.D. degree. After internship in Norway, he moved to the USA for education in surgery. He was a Specialist in general surgery, in 1981, and cardiothoracic surgery, in 1983, the Director of Cardiac Surgery, Buffalo VA Hospital, the Director of the Cardiac Transplantation Program, Buffalo General Hospital, the Director of the Center for Less Invasive Cardiac Surgery, a Clinical Associate Professor of Surgery, The State University of New York at Buffalo, an Initiator of the hospital partnership between Buffalo General Hospital and the Tuzla Medical Center, Bosnia, in 1995, and a Developer of Cardiovascular Surgery and Cardiology, Bosnia and Herzegovina. He is currently a Researcher and a Co-Investigator with The Intervention Centre, Oslo University Hospital, the Medical Director of the BH Heart Centre, Tuzla BIH, and the Medical Director of Medical Device Company, Cardiomech AS.

ILANGKO BALASINGHAM (SM'12) received the M.Sc. and Ph.D. degrees in signal processing from the Department of Electronics and Telecommunications, Norwegian University of Science and Technology (NTNU), Trondheim, Norway, in 1993 and 1998, respectively. He performed the master's degree thesis with the Department of Electrical and Computer Engineering, University of California at Santa Barbara, Santa Barbara, CA, USA. From 1998 to 2002, he was a Research Engineer developing image and video streaming solutions for mobile handheld devices with the Fast Search and Transfer ASA, Oslo, Norway, which is now a part of Microsoft Inc. Since 2002, he has been a Senior Research Scientist with the Intervention Center, Oslo University Hospital, Oslo, where he heads the Wireless Sensor Network Research Group. He was appointed as a Professor in signal processing in medical applications with NTNU, in 2006. From 2016 to 2017, he was a Professor by courtesy with the Frontier Institute, Nagoya Institute of Technology, Japan. He has authored or coauthored more than 200 journals and conference papers, seven book chapters, 42 abstracts, five patents, and 16 articles in popular press. His research interests include super robust short range communications for both inbody and onbody sensors, body area sensor network, microwave short range sensing of vital signs, short range localization and tracking mobile sensors, and nanoscale communication networks. He has given 16 invited/keynotes at the international conferences. In addition, he is active in organizing conferences (Steering Committee Member of ACM NANOCOM, from 2018 to 2021, the General Chair: the 2019 IEEE International Symposium of Medical ICT and the 2012 Body Area Networks Conference, and the TPC Chair of the 2015 ACM NANOCOM), and an Editorial Board (has been an Area Editor of *Nano Communication Networks* (Elsevier), since 2013).